ELSEVIER

2015 International Congress on Ultrasonics, 2015 ICU Metz

A numerically efficient damping model for acoustic resonances in microfluidic cavities

Philipp Hahn*, Jurg Dual

Institute of Mechanical Systems (IMES), ETH Zurich, Tannenstr. 3, CH-8092 Zrich, Switzerland

Abstract

Acoustofluidic damping is a crucial factor that limits the attainable acoustic amplitudes and therefore the effectiveness of acoustofluidic devices. It can be traced back to viscous and thermal dissipation in the bulk and in the boundary layers at cavity walls or suspended particles. However, numerical 3D simulations that include all relevant physics are prohibitively expensive since the acoustic boundary layers need to be resolved. We present a way to incorporate the dissipation effects into a synthetic acoustofluidic loss factor for the use in 3D device simulations. It comes at minimum numerical cost since boundary layers are resolved analytically. Our results and the validity of the physical assumptions we make in the derivation have been verified by analytical and numerical reference solutions. The acoustofluidic loss factor is easily incorporated in device models for a numerically feasible and quantitatively accurate prediction of acoustic amplitudes. In this sense, our work represents the missing link that allows to make not only qualitative but also quantitative predictions of acoustofluidic forces in realistic 3D devices.

1. Introduction

Operating in the low MHz regime, bulk acoustic wave (BAW) devices are an emerging technology for the contactless and cost effective handling of cells, bacteria and other micro-particles. A comprehensive review of theoretical work, experimental setups as well as recent developments can be found in the book "Microscale Acoustofluidics" (Laurell and Lenshof (2015)). BAW devices are typically driven in a resonant state to achieve enhanced acoustic amplitudes and high acoustofluidic forces for the manipulation of micro-particles. Among other loss mechanisms related to the structural parts of acoustofluidic devices, losses in the fluid, termed *acoustofluidic damping*, crucially affect the attainable acoustic amplitudes. In typical micro-devices, these losses are mainly caused by the thin viscous boundary layer (approx. $0.5\,\mu$m at 1 MHz in water) at the fluid cavity walls and suspended particles. Even with modern computing hardware at hand, it is prohibitively expensive to resolve these boundary layers in 3D numerical device models.

---

* Corresponding author. Tel.: +41 44 633 92 37
  E-mail address: hahnp@ethz.ch

However, in the bulk of the fluid cavity, the viscous boundary layer hardly affects the first-order time-harmonic field in a qualitative fashion. It rather defines its amplitude at resonance by the induced damping. For this reason, the boundary layers can be omitted from device models as long as their dissipative effect is retained. The same applies for the thermal boundary layers.

The traditional way to model ultrasonic wave attenuation due to dissipation in the bulk of the fluid is to use a complex speed of sound as a function of the loss factor φ (Kinsler et al. (2000)). It can be shown that the associated power loss is $\Psi_{\text{bulk}} = \omega\varphi W_{\text{st}}$, where ω is the angular frequency and W_{st} is twice the stored time-averaged potential energy in the fluid. In our novel approach, we calculate and summarize the dissipation associated with each acoustofluidic loss mechanism to define a synthetic loss coefficient $\bar{\varphi}(f)$ that we call the *acoustofluidic loss factor* (Hahn and Dual (2015)). We account for all acoustofluidic losses (*e.g.* viscous boundary layer damping) by calculating the complex speed of sound c according to,

$$c(f) = c_0\left(1 + \mathrm{i}\frac{\bar{\varphi}(f)}{2}\right), \quad \text{with} \quad \bar{\varphi}(f) = \sum_n \bar{\varphi}_n(f) = \frac{\sum_n \Psi_n(f)}{\omega W_{\text{st}}(f)}, \tag{1}$$

where c_0 is the real-valued speed of sound of the fluid and each n in the summation is associated with one loss mechanism and the corresponding power dissipation $\Psi_n(f)$. The main difficulty is to calculate $\Psi_n(f)$ in a physically accurate way. Omitting explicit frequency dependence $\ldots(f)$ from here on, we emphasize that all terms depend on the frequency f and, therefore, on the mode considered. Throughout this paper, we assume the fluid to be water at room temperature and we refer to Muller and Bruus (2014) as well as Hahn and Dual (2015) for detailed properties.

2. Losses in BAW micro-devices

The critical reader might question if acoustofluidic damping is really important in the context of other losses associated with glue layers, structural parts of the device, or the energy transfer into the device support (anchor loss). Certainly, there are examples where devices are clamped or glued to large structures and anchor losses are dominant. However, the device is placed on a low-impedance base made of foam or tissue paper, the anchor losses become negligible. For this scenario, we analyze the energy distribution inside a typical silicon-based BAW device, quantifying the losses in each device component. As often in experiments, the device is piezo-electrically excited at a frequency that leads to a strong time-harmonic field in the fluid cavity. The 3D device model contains a silicon device body, a glass lid, a piezoelectric transducer, and a glue layer between the transducer and the silicon (Hahn et al. (2014)). The device geometry and the potential energy density at 0.84 MHz are illustrated in Fig. 1. For the
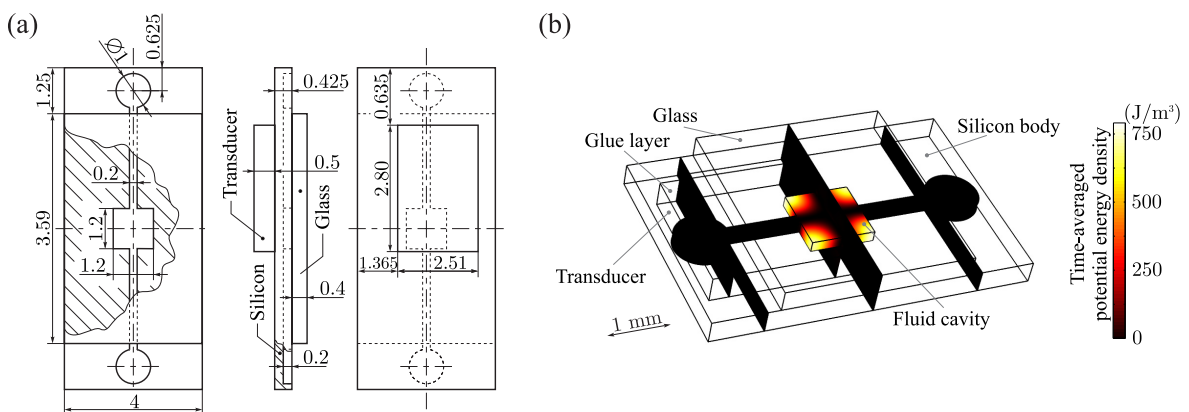

Fig. 1. (a) BAW device geometry as drawn in a top view, in a side view, and in a bottom view. (b) Energy distribution in the device for excitation at 0.84 MHz and 5 Vpp. Shown is the time-averaged acoustic potential energy density in the water and the time-averaged strain energy density on three cut planes through the device structure. Energy is focused on the fluid cavity.

calculation of the stored energy W_{st} and the power dissipation Ψ in Table 1 we refer to Hahn and Dual (2015), whereas

the acoustofluidic loss factor is chosen as outlined in section 3 to account for all losses in the fluid cavity. The data shows that over 50% of the total loss are related to acoustofluidic dissipation.

Table 1. Stored energy and power dissipation in the acoustofluidic micro-device according to Fig. 1 with excitation at 0.84 MHz and 5 Vpp. Values are provided for all individual device components as well as for the summation over the whole device. The power dissipation in the piezoelectric transducer contains mechanical, dielectric, and piezoelectric losses.

Parameter	Symbol	Transducer	Silicon	Glass	Glue	Water	$\sum$ Device	Unit
Stored energy	W_{st}	10.4	15.4	8.9	2.6	105.9	143.2	nJ
Power dissipation	Ψ	0.53	0	0.02	1.36	2.24	4.15	mW

3. Acoustofluidic loss factor

As outlined in eq. 1, the acoustofluidic loss factor $\bar{\varphi}$ can be written as the sum of individual components $\bar{\varphi}_n$, each related to a physical dissipation effect in the fluid cavity. Specifically, these effects are (Hahn and Dual (2015)):

- viscous ($\bar{\varphi}_1$) and thermal ($\bar{\varphi}_2$) damping in the bulk
- viscous ($\bar{\varphi}_3$)and thermal ($\bar{\varphi}_4$) damping at the cavity walls
- viscous ($\bar{\varphi}_5$) and thermal ($\bar{\varphi}_6$)damping due to suspended particles
- nonlinear effects *i.e.* radiation forces ($\bar{\varphi}_7$) and acoustic streaming ($\bar{\varphi}_8$)

It can be shown that thermal dissipation effects ($\bar{\varphi}_2$, $\bar{\varphi}_4$, $\bar{\varphi}_6$) are at least two orders of magnitude smaller than their viscous counterparts ($\bar{\varphi}_1$, $\bar{\varphi}_3$, $\bar{\varphi}_5$) and that the boundary layer losses dominate at typical operation frequencies and cavity sizes (Hahn and Dual (2015)). Nonlinear losses are neglected because the acoustic amplitudes are small. For this reason, we focus on the viscous boundary layer losses at cavity walls and suspended particles.

3.1. Viscous boundary layer damping at cavity walls

The tangential relative velocity between the structural wall vibration and the time-harmonic fluid motion outside the boundary layer leads to viscous shear and dissipation (Hahn and Dual (2015); Swift (1988)). The associated loss factor component φ_3 can be written as

$$\varphi_3 = \frac{\rho_0 \delta}{4 W_{st}} \int_S |\xi_{\text{diff}i}|^2 \mathrm{d}S, \tag{2}$$

with the viscous penetration depth δ and the tangential relative velocity vector $\xi_{\text{diff}i}$ in index notation. The integration is carried out over the cavity surface S. Besides the frequency dependent δ, the expression also includes W_{st} and the integral which both display a complex dependence on the acoustic mode shape and the vibrating cavity walls. A comparison with analytical and numerical reference simulations showed that eqn. 2 delivers accurate results, even if the cavity geometry is complex or if the viscous boundary layer is relatively thick (Hahn and Dual (2015)).

3.2. Viscous boundary layer damping at suspended particles

A particle density that is different from the water density gives rise to viscous shear and dissipation around the particle, as analogous to the case above. For elastic spherical particles, much smaller than the acoustic wavelength, there exists an analytic solution of the time-harmonic fluid motion in the vicinity of the particle (Settnes and Bruus (2012)). The associated viscous dissipation due to *one* suspended particle can be calculated based on this solution. For a given volumetric particle concentration C (which may depend on position but it needs to be small enough to neglect particle-particle interaction), the associated acoustofluidic loss factor component reads,

$$\varphi_5 = \frac{A}{V_p \omega W_{st}} \int_V C |v_i|^2 \mathrm{d}V, \tag{3}$$

where

$$A = \frac{48 a^5 (a + \delta) \eta \pi (-1 + \tilde{\rho})^2}{\delta (162 a^2 \delta^2 + 162 a \delta^3 + 81 \delta^4 + 4 a^4 (1 + 2\tilde{\rho})^2 + 36 a^3 (\delta + 2\delta\tilde{\rho}))}, \tag{4}$$

and $\tilde{\rho} = \rho_p/\rho_0$ with the particle density ρ_p, the particle radius a, the spherical particle volume V_p, and the undisturbed time-harmonic fluid velocity vector v_i in index notation. The integration in eq. 3 is performed over the fluid volume V. The expression strongly depends on the acoustic mode shape in the fluid cavity as well as the particle distribution. At identical particle and fluid density ($\tilde{\rho} = 1$), the loss factor component φ_5 vanishes. The results of eqn. 2 have been validated against numerical reference simulations that directly resolve the viscous boundary layer. Remarkable agreement within a fraction of 1% has been found in all studied examples (Hahn and Dual (2015)).

4. Acoustofluidic loss factor in a realistic BAW micro-device

For the device shown in Fig. 1 (a), we evaluate the acoustofluidic loss factor with all its components for the frequency range between 0.1 MHz and 2 MHz. Since the loss factor components of section 3 depend on the acoustic mode shape in the fluid cavity, they cannot be calculated *a priori*. Nevertheless, they can be determined based on a preceding device simulation where the acoustofluidic loss factor is only roughly guessed. Based on these simulation results, the realistic acoustofluidic loss factor can be calculated and plugged into the final device simulation which then is able to predict the amplitudes accurately. This procedure works because a wrong acoustofluidic loss factor only scales the simulation results with no effect on the derived loss factor components. Figure 2 shows that the acoustofluidic loss factor can vary dramatically with frequency and confirms that the viscous boundary layer related terms dominate.
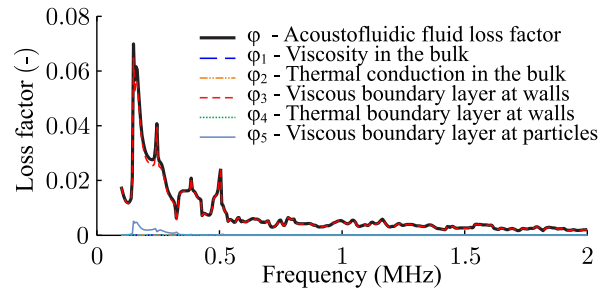

Fig. 2. Acoustofluidic loss factor and its individual components in a realistic 3D BAW device simulation (see Fig. 1). Some loss factor components are too small to be visible. Results are shown for a uniform 0.1 volume-% of particles ($\tilde{\rho} = 0.6$, $a = 10\,\mu$m).

5. Conclusion

We have demonstrated the significance and calculation of the acoustofluidic loss factor in 3D BAW devices. Our numerical device model is computationally efficient and allows a quantitative prediction of the acoustic amplitudes inside realistic BAW devices. With augmentations, the model can accurately predict the acoustic radiation forces on particles as well as the acoustic streaming velocities inside acoustofluidic cavities.

References

Hahn, P., Dual, J., 2015. A numerically efficient damping model for acoustic resonances in microfluidic cavities. Submitted to Physics of Fluids .
Hahn, P., Schwab, O., Dual, J., 2014. Modeling and optimization of acoustofluidic micro-devices. Lab Chip 14, 3937–3948.
Kinsler, L.E., Frey, A.R., Coppens, A.B., Sanders, J.V., 2000. Fundamentals of Acoustics. 2 ed., Wiley, New York.
Laurell, T., Lenshof, A. (Eds.), 2015. Microscale Acoustofluidics. Royal Society of Chemistry, Cambridge, UK.
Muller, P.B., Bruus, H., 2014. Numerical study of thermoviscous effects in ultrasound-induced acoustic streaming in microchannels. Phys. Rev. E 90, 043016.
Settnes, M., Bruus, H., 2012. Forces acting on a small particle in an acoustical field in a viscous fluid. Phys. Rev. E 85, 016327.
Swift, G.W., 1988. Thermoacoustic engines. J. Acoust. Soc. Am. 84, 1145–1180.